

Dyades of Coproporphyrin I with Porphyrinoids Bound by Azine Bridge

Alena O. Shkirdova, Vladimir S. Tyurin,[@] and Ilya A. Zamilatskov[@]

A.N. Frumkin Institute of Physical Chemistry and Electrochemistry, Russian Academy of Sciences, 119071 Moscow, Russia
[@]Corresponding author E-mail: vst-1970@mail.ru, joz@mail.ru

Dedicated to Academician Irina P. Beletskaya on the occasion of her Anniversary

New asymmetric dyads consisting of porphyrin and chlorin components connected by an azine bridge have been obtained. Nickel and palladium complexes of tetramethyl ester of coproporphyrin I were used as porphyrin components, and chlorin was represented by methyl esters of pyropheophorbide a and d. Mesohydrzones of Ni^{II} and Pd^{II} complexes of the coproporphyrin I tetraethyl ester reacted with methyl pyropheophorbide a and methyl pyropheophorbide d resulting in the formation of dyads with good yields. Photophysical studies of dyads showed that in the ground state there is a weak interaction between the components. In this case, the interaction is enhanced in the excited state. DFT calculations showed the orthogonality of the orientation of the azine bridge with respect to the porphyrin ring in the ground state and the presence of conjugation in the excited state.

Keywords: Porphyrins, chlorins, dyads, azines, singlet oxygen generation, photosensitizers.

Диады копропорфирина I с пиррофеофорбидами, связанные азиновым мостиком

А. О. Шкирдова, В. С. Тюрин,[@] И. А. Замилацков[@]

Институт физической химии и электрохимии им. А.Н. Фрумкина РАН, 119071 Москва, Российская Федерация
[@]E-mail: vst-1970@mail.ru, joz@mail.ru

Посвящается Академику Ирине Петровне Белецкой по случаю ее юбилея

Получены новые несимметричные диады, состоящие порфиринового и хлоринового компонентов, связанных азиновым мостиком. В качестве порфириновых компонентов использовали никелевый и палладиевый комплексы тетраэтилового эфира копропорфирина I, а хлорин был представлен метиловыми эфирами пиррофеофорбида a и d. Мезогидразоны комплексов Ni^{II} и Pd^{II} тетраэтилового эфира копропорфирина I вступают в реакцию с метил пиррофеофорбидами a и d, что приводит к образованию диад с хорошими выходами. Фотофизические исследования диад показали, что в основном состоянии наблюдается слабое взаимодействие между компонентами. При этом взаимодействие усиливается в возбужденном состоянии. DFT расчеты показали ортогональность ориентации азинового мостика по отношению к порфириновому кольцу в основном состоянии и наличие сопряжения в возбужденном состоянии.

Ключевые слова: Порфирины, хлорины, диады, азины, фотосенсибилизаторы, образование синглетного кислорода.

Introduction

Porphyrins are at focus of many research areas. Like the photosynthesis reaction center, many artificial systems use both symmetrical porphyrin dimers and asymmetric

dyads as photosensitizers in photovoltaics,^[1] photocatalytic hydrogen production,^[2] in photodynamic therapy for cancer treatment, optoelectronic devices.^[3-8] They are also used as catalysts,^[9] sensors,^[10,11] building blocks for supramolecular ensembles, and molecular devices and machines.^[12] Also

many porphyrins come from natural sources, now majority of the tetrapyrrole compounds are fully synthetic, starting from tetrapyrrole condensation.^[13] Subsequent functionalization allows to build porphyrin molecules with the functional groups necessary to bind components into dyads.^[14-16]

Porphyrin dyads containing structural fragments with different electronic energies and redox properties can undergo energy or electron transfer in excited state. The nature of the connecting bridge may have a dramatic influence on these processes of energy and electron transfer. The bridge in porphyrin dyads plays a critical role in determining the electronic properties of the molecule and photophysical behavior of the substance. It affects the energy transfer between the two porphyrin units, the stability of the dyad, and the overall redox properties of the molecule. The choice of bridge can also determine the potential applications of the porphyrin dyad, such as in the design of organic solar cells or other optoelectronic devices. Therefore, the synthesis of asymmetric porphyrin dyads with certain excitation energy parameters and redox potentials, as well as various types of connecting bridges, is of great interest for the development of new molecular structures. Among various types of bridges azine bridges are among least studied to date. Azine group is formed by condensation of two carbonyl groups (aldehyde or ketone) with hydrazine. Compounds, containing the azine group, feature distinctive structural and electronic features and may be used as dyes,^[17] sensors,^[18,19] aggregation-induced fluorophores,^[20] NLO and optoelectronic materials,^[21,22] organic field-effect transistors (OFETs),^[23,24] potential antiviral and antitumor agents,^[25,26] luminescent liquid crystals.^[27] Conjugated polymeric azines were reported for electronic, optoelectronic, and photonic applications.^[24,28,29] Azines are isoelectronic analogues of 1,3-butadiene,^[30] however, they differ significantly from 1,3-butadiene with respect to conjugation.^[31] In some cases, azines can be conductors of conjugation of π -electrons of the fragments they connect, and in others azines can broke the conjugation chain. Previously, we have developed methods for the synthesis and investigated properties of porphyrin dyads connected both by the 1,3-butadiene^[32] and the azine bridges.^[33,34] In continuation of these studies, new types of asymmetric porphyrin-chlorin dyads linked with azine bridge were obtained in this work, consisting of metal complexes of coproporphyrin I connected to the free bases of pyropheophorbide *a* and pyropheophorbide *d*.

Experimental

General

Reactions were carried out under argon atmosphere using commercially available reagents that were purchased and used as received. Heating reaction vessels was performed with oil bath. Silica gel 40/60 was used for column and flash chromatography. Preparative thin layer chromatography (TLC) was performed using glass plates coated with 5-40 μm silica gel (5 mm thick). ¹H and ¹³C NMR spectra were recorded with a Bruker Avance III 600 MHz spectrometer at 303 K in CDCl₃. Chemical shifts are reported relative to signals of residual protons of solvents (CDCl₃ – 7.26 ppm). The assignment of the resonances in the ¹H NMR spectra was achieved by the use of COSY and HSQC techniques. The LDI-TOF mass-spectra were obtained on a Ultraflex-II mass spectrometer (Bruker Daltonics) in a positive ion mode using

reflection mode (20 mV target voltage) without matrix. Electronic absorption spectra were recorded with U-2900 (Hitachi) spectrophotometer in quartz rectangular cells of 10 mm path length.

Synthesis

Methyl pyropheophorbide *a* was obtained from commercial sources. Methyl pyropheophorbide *d* was obtained *via* oxidation of methyl pyropheophorbide *a* using reported procedures.^[35,36] Tetraethyl ester of the coproporphyrin I (3,8,13,18-tetramethyl-2,7,12,17-tetra(2-(ethoxycarbonyl)ethyl)porphyrin) was synthesized according to a procedure, developed by K. Smith,^[37] modified by use of ethanol instead of methanol. Ni^{II} complex of the tetraethyl ester of the coproporphyrin I (1) and Ni^{II} complex of tetraethyl ester of hydrazone of *meso*-formyl coproporphyrin I [(*E*)-1-(3,8,13,18-tetramethyl-2,7,12,17-tetra(2-(ethoxycarbonyl)ethyl)-porphyrinatonicel-5-yl)methylene]hydrazine, 3] were synthesized from the corresponding tetraethyl ester of the coproporphyrin I according to the published procedures.^[38]

3,8,13,18-Tetramethyl-2,7,12,17-tetra(2-(ethoxycarbonyl)ethyl)porphyrinatopalladium (2) was prepared via modified procedure of Adler and Longo.^[39] PdCl₂ (164 mg, 0.93 mmol) was dissolved at heating in 15 mL of DMF and the resulted solution was added to a solution of tetraethyl ester of the coproporphyrin I (142 mg, 0.19 mmol) in 15 mL of DMF, then NaOAc (106 mg, 1.30 mmol) was added and the mixture was stirred for 12 hrs at 150 °C. After that the reaction mixture was poured into ice water (0.15 L) and the precipitate was filtered, dissolved in 20 mL of CH₂Cl₂, washed with water (2×10 mL), dried over Na₂SO₄, evaporated in vacuum, and the product was purified by flash chromatography with CH₂Cl₂/EtOH 100:1 (R_f = 0.28) yielding 121 mg (75 %) of the product 2. ¹H NMR (600 MHz, CDCl₃, 303 K) δ ppm: 1.19 (12H, t, *J* = 7.17 Hz, OCH₂CH₃), 3.27 (8H, m, CH₂CO₂Et), 3.63 (12H, s, β -CH₃), 4.21 (8H, q, *J* = 7.17 Hz, OCH₂CH₃), 4.38 (8H, m, CH₂CH₂CO₂Et), 10.07 (4H, s, *meso*-CH). LDI TOF *m/z*: found 871.29, calc. for [M+H]⁺ C₄₄H₅₃N₄O₈Pd 871.2893. UV-Vis (CH₂Cl₂) λ_{max} (A_{rel.}) nm: 392 (1.00), 511 (0.08), 546 (0.23).

(*E*)-((3,8,13,18-Tetramethyl-2,7,12,17-tetra(2-(ethoxycarbonyl)ethyl)porphyrinatopalladium-5-yl)methylene)hydrazine (4) was obtained via the modified one-pot procedure^[38] of the Vilsmeier-Haack formylation reaction^[40] followed by the interaction of the intermediate “phosphorus complex” with hydrazine. The Vilsmeier reagent, prepared from POCl₃ (1 mL, 10.7 mmol) and N,N-dimethylformamide (1 mL, 12.9 mmol), was added dropwise to a rapidly stirred solution of Pd^{II} complex of the tetraethyl ester of the coproporphyrin I (2) (50 mg, 0.057 mmol) in 10 mL of dry 1,2-dichloroethane at 90 °C. The resulting mixture was stirred for 3 hrs at 90 °C, then the solvent was evaporated in vacuum and the residue was dissolved in CH₂Cl₂ (50 mL) and washed with H₂O (50 mL), then dried over sodium sulfate. The solution was concentrated in vacuum to the volume of 30 mL and 0.1 mL of hydrazine hydrate was added and the completion of the reaction was checked by TLC (CH₂Cl₂/EtOH 100:1). Then the reaction mixture was washed with water (2×10 mL), dried over sodium sulfate, the solvent was evaporated in vacuum, and the residue was purified by column chromatography (silica gel) with eluent CH₂Cl₂/EtOH 100:1 (R_f = 0.18) to afford 35 mg (67 %) of the Pd^{II} complex of *meso*-hydrazone derivative of coproporphyrin I tetraethyl ester (4). ¹H NMR (CDCl₃, 278 K) δ_{H} ppm: 1.19 (6H, t, *J* = 7.20 Hz, OCH₂CH₃), 1.22 (3H, t, *J* = 7.11 Hz, OCH₂CH₃), 1.35 (3H, t, *J* = 7.20 Hz, OCH₂CH₃), 1.62 (2H, s, NH₂), 2.92 (2H, m, CH₂CO₂Et), 3.12 (2H, m, CH₂CO₂Et), 3.19 (7H, m, CH₂CO₂Et, β -CH₃), 3.48 (3H, s, β -CH₃), 3.49 (3H, s, β -CH₃), 3.51 (3H, s, β -CH₃), 4.02 (2H, m, CH₂CH₂CO₂Et), 4.21 (12H, m, CH₂CH₂CO₂Et, OCH₂CH₃), 4.28 (2H, q, *J* = 7.20 Hz, OCH₂CH₃), 9.74 (1H, s, 15-CH), 9.81 (1H, s, 20-CH), 9.86 (1H, s, 10-CH),

10.78 (1H, s, CH=N). LDI TOF m/z : found 913.38, calc. for $[M+H]^+$ $C_{45}H_{55}N_6O_8Pd$: 913.31. UV-Vis (CH_2Cl_2) λ_{max} ($A_{rel.}$) nm: 399 (1.00), 516 (0.09), 550 (0.18).

(1E,2E)-1-(Methylpyropheophorbide d-3¹-ylidene)-2-((3,8,13,18-tetramethyl-2,7,12,17-tetra(2-(ethoxycarbonyl)ethyl)-porphyrinatonicel-5-yl)methylene)hydrazine (5). Ni^{II} complex **3** (34 mg, 0.039 mmol) and methyl pyropheophorbide *d* (22 mg, 0.039 mmol) were dissolved in 5 mL of CH_2Cl_2 , and 13 μ L of 0.32 M solution of trifluoroacetic acid in CH_2Cl_2 was added. The reaction mixture was stirred and refluxed for 24 hours, then concentrated in vacuum and purified using preparative TLC in $CH_2Cl_2/EtOH$ 50:1 (R_f = 0.28), yielding 25 mg (46%) of the dyad **5**. 1H NMR ($CDCl_3$, 278 K) δ_H ppm: -1.78 (1H, s, NH), 0.12 (1H, s, NH), 0.68 (3H, t, J = 7.13 Hz, OCH_2CH_3), 1.26 (9H, m, OCH_2CH_3), 1.76 (3H, t, J = 7.64 Hz, 8^2-CH_3), 1.88 (3H, d, J = 7.5 Hz, 18^1-CH_3), 2.35 (2H, m, 17^1-CH^b , 17^2-CH^b), 2.63 (1H, m, 17^2-CH^a), 2.76 (1H, m, 17^1-CH^a), 3.13 (2H, m, CH_2CO_2Et), 3.17 (4H, m, CH_2CO_2Et), 3.21 (2H, m, CH_2CO_2Et), 3.43 (3H, s, $\beta-CH_3$ – coproporphyrin part), 3.46 (3H, s, $\beta-CH_3$ – coproporphyrin part), 3.47 (3H, s, 7^1-CH_3 – pyropheophorbide part), 3.49 (3H, s, OCH_3), 3.58 (3H, s, 2^1-CH_3 – pyropheophorbide part), 3.66 (3H, s, 12^1-CH_3 – pyropheophorbide part), 3.70 (8H, m, OCH_2CH_3 , $\beta-CH_3$ – coproporphyrin part), 3.75 (2H, m, OCH_2CH_3), 4.22 (12H, m, OCH_2CH_3 , $CH_2CH_2CO_2Et$, 8^1-CH_2 – pyropheophorbide part), 4.32 (2H, m, $CH_2CH_2CO_2Et$), 4.37 (1H, m, 17-CH), 4.56 (1H, m, 18-CH), 5.18 (1H, d, J = 19.47 Hz, 13^2-CH^b), 5.32 (1H, d, J = 19.47 Hz, 13^2-CH^a), 8.75 (1H, s, 20-CH – pyropheophorbide part), 9.54 (1H, s, 15-CH – coproporphyrin part), 9.57 (1H, s, 20-CH – coproporphyrin part), 9.58 (1H, s, 10-CH – coproporphyrin part), 9.63 (1H, s, 10-CH – pyropheophorbide part), 9.99 (1H, s, 5-CH – pyropheophorbide part), 10.55 (1H, s, CH=N – pyropheophorbide part). LDI TOF m/z : found 1397.30, calc. for $[M+H]^+$ $C_{78}H_{87}N_{10}O_{11}Ni$ 1397.59. UV-Vis (CH_2Cl_2) λ_{max} ($A_{rel.}$) nm: 404 (1.00), 430 (0.68), 523 (0.18), 557 (0.22), 633 (0.08), 695 (0.53).

(1E,2E)-1-(Methylpyropheophorbide d-3¹-ylidene)-2-((3,8,13,18-tetramethyl-2,7,12,17-tetra(2-(ethoxycarbonyl)ethyl)-porphyrinatopalladium-5-yl)methylene)hydrazine (6). Pd^{II} complex **4** (31 mg (0.034 mmol) and methyl pyropheophorbide *d* (19 mg, 0.034 mmol) were dissolved in 5 mL of CH_2Cl_2 , and 22 μ L of 0.32 M solution of trifluoroacetic acid in CH_2Cl_2 was added. The reaction mixture was stirred and refluxed for 48 hours, then concentrated in vacuum and purified using preparative TLC in $CH_2Cl_2/EtOH$ 50:1 (R_f = 0.25), yielding 22 mg (44%) of the dyad **6**. 1H NMR ($CDCl_3$, 278 K) δ_H ppm: -1.93 (1H, s, NH), 0.12 (1H, s, NH), 0.56 (3H, t, J = 7.17 Hz, OCH_2CH_3), 1.21 (9H, m, OCH_2CH_3), 1.69 (3H, t, J = 7.66 Hz, 8^2-CH_3), 1.98 (3H, d, J = 7.37 Hz, 18^1-CH_3), 2.36 (2H, m, 17^1-CH^b и 17^2-CH^b), 2.63 (1H, m, 17^2-CH^a), 2.77 (1H, m, 17^1-CH^a), 3.13 (2H, m, CH_2CO_2Et), 3.21 (2H, m, CH_2CO_2Et), 3.30 (4H, m, CH_2CO_2Et), 3.50 (6H, s, $\beta-CH_3$ – coproporphyrin part), 3.55 (2H, m, OCH_2CH_3), 3.59 (3H, s, $\beta-CH_3$ – coproporphyrin part), 3.64 (3H, s, 7^1-CH_3 – pyropheophorbide part), 3.65 (3H, s, 2^1-CH_3 – pyropheophorbide part), 3.67 (3H, s, 12^1-CH_3 – pyropheophorbide part), 3.80 (3H, m, $\beta-CH_3$ – coproporphyrin part), 4.11 (2H, m, $CH_2CH_2CO_2Et$), 4.23 (6H, m, OCH_2CH_3), 4.40 (10H, m, OCH_3 , 17-CH, $CH_2CH_2CO_2Et$), 4.58 (1H, m, 18-CH), 5.15 (1H, d, J = 19.62 Hz, 13^2-CH^b), 5.29 (1H, d, J = 19.62 Hz, 13^2-CH^a), 8.79 (1H, s, 20-CH – pyropheophorbide part), 9.18 (1H, s, 15-CH – coproporphyrin part), 9.81 (1H, s, 20-CH – coproporphyrin part), 10.02 (1H, s, 10-CH – coproporphyrin part), 10.06 (1H, s, 10-CH – pyropheophorbide part), 10.27 (1H, s, 5-CH – pyropheophorbide part), 10.70 (1H, s, CH=N – pyropheophorbide part), 11.71 (1H, s, CH=N – coproporphyrin part). LDI TOF m/z : found 1445.03, calc. for $[M+H]^+$ $C_{78}H_{87}N_{10}O_{11}Pd$ 1445.56. UV-Vis (CH_2Cl_2) λ_{max} ($A_{rel.}$) nm: 403 (1.00), 429 (0.67), 520 (0.22), 552 (0.31), 633 (0.08), 694 (0.47).

(1E,2E)-1-(Methylpyropheophorbide a-13¹-ylidene)-2-((3,8,13,18-tetramethyl-2,7,12,17-tetra(2-(ethoxycarbonyl)ethyl)-porphyrinatonicel-5-yl)methylene)hydrazine (7). Ni^{II} complex **3** (32 mg, 0.037 mmol) and methyl pyropheophorbide *a* (20 mg, 0.037 mmol) were dissolved in 5 mL of CH_2Cl_2 , and 23 μ L of 0.32 M solution of trifluoroacetic acid in CH_2Cl_2 was added. The reaction mixture was stirred and refluxed for 24 hours, then concentrated in vacuum and purified using preparative TLC in $CH_2Cl_2/EtOH$ 50:1 (R_f = 0.23), yielding 29 mg (56%) of the dyad **7**. 1H NMR ($CDCl_3$, 278 K) δ_H ppm: -2.50 (1H, s, NH), 0.11 (1H, s, NH), 0.43 (3H, t, J = 7.18 Hz, OCH_2CH_3), 1.23 (3H, t, J = 7.10 Hz, OCH_2CH_3), 1.25 (6H, m, OCH_2CH_3), 1.64 (3H, d, J = 7.33 Hz, 18^1-CH_3), 1.81 (3H, t, J = 7.69 Hz, 8^2-CH_3), 1.96 (1H, m, 17^2-CH^b), 2.04 (1H, m, 17^1-CH^b), 2.19 (1H, m, 17^2-CH^a), 2.33 (1H, m, 17^1-CH^a), 2.98 (3H, s, $\beta-CH_3$ – coproporphyrin part), 3.12 (2H, m, CH_2CO_2Et), 3.17 (6H, m, CH_2CO_2Et), 3.37 (3H, s, $\beta-CH_3$ – coproporphyrin part), 3.48 (3H, s, $\beta-CH_3$ – coproporphyrin part), 3.49 (3H, s, 7^1-CH_3 – pyropheophorbide part), 3.50 (3H, s, 2^1-CH_3 – pyropheophorbide part), 3.53 (3H, s, 12^1-CH_3 – pyropheophorbide part), 3.68 (2H, m, OCH_2CH_3), 3.86 (2H, q, J = 7.69 Hz, 8^1-CH_2 – pyropheophorbide part), 3.99 (3H, s, OCH_3), 4.00 (1H, m, 17-CH), 4.22 (14H, m, OCH_2CH_3 , $CH_2CH_2CO_2Et$), 4.38 (1H, m, 18-CH), 5.27 (1H, d, J = 19.66 Hz, 13^2-CH^b), 5.37 (1H, d, J = 19.66 Hz, 13^2-CH^a), 6.18 (1H, d, J = 11.55 Hz, 3^2-CH^b), 6.32 (1H, d, J = 17.78 Hz, 3^2-CH^a), 8.13 (1H, dd, J_1 = 17.78 Hz, J_2 = 11.55 Hz, 3^1-CH), 8.66 (1H, s, 20-CH – pyropheophorbide part), 9.62 (1H, s, 15-CH – coproporphyrin part), 9.64 (1H, s, 20-CH – coproporphyrin part), 9.66 (1H, s, 10-CH – coproporphyrin part), 9.67 (1H, s, 10-CH – pyropheophorbide part), 9.73 (1H, s, 5-CH – pyropheophorbide part), 11.34 (1H, s, CH=N). LDI TOF m/z : found 1395.33, calc. for $[M+H]^+$ $C_{79}H_{89}N_{10}O_{10}Ni$ 1395.61. UV-Vis (CH_2Cl_2) λ_{max} ($A_{rel.}$) nm: 403 (1.00), 514 (0.19), 561 (0.15), 623 (0.09), 682 (0.53).

(1E,2E)-1-(Methylpyropheophorbide a-13¹-ylidene)-2-((3,8,13,18-tetramethyl-2,7,12,17-tetra(2-(ethoxycarbonyl)ethyl)-porphyrinatopalladium-5-yl)methylene)hydrazine (8). Pd^{II} complex **4** (28 mg, 0.031 mmol) and methyl pyropheophorbide *a* (17 mg, 0.031 mmol) were dissolved in 5 mL of CH_2Cl_2 , and 20 μ L of 0.32 M solution of trifluoroacetic acid in CH_2Cl_2 was added. The reaction mixture was stirred and refluxed for 72 hours, then concentrated in vacuum and purified using preparative TLC in $CH_2Cl_2/EtOH$ 50:1 (R_f = 0.22), yielding 19 mg (43%) of the dyad **8**. 1H NMR ($CDCl_3$, 278 K) δ_H ppm: -2.40 (1H, s, NH), 0.11 (1H, s, NH), 0.31 (3H, t, J = 7.10 Hz, OCH_2CH_3), 1.21 (9H, m, OCH_2CH_3), 1.66 (3H, d, J = 7.51 Hz, 18^1-CH_3), 1.85 (3H, t, J = 7.79 Hz, 8^2-CH_3), 2.09 (2H, m, 17^1-CH^b , 17^2-CH^b), 2.23 (1H, m, 17^2-CH^a), 2.42 (1H, m, 17^1-CH^a), 2.93 (3H, s, $\beta-CH_3$ – coproporphyrin part), 3.23 (4H, m, CH_2CO_2Et), 3.31 (4H, m, CH_2CO_2Et), 3.39 (3H, s, 2^1-CH_3 – pyropheophorbide part), 3.47 (3H, s, 12^1-CH_3 – pyropheophorbide part), 3.54 (2H, q, J = 7.10 Hz, OCH_2CH_3), 3.55 (3H, s, $\beta-CH_3$ – coproporphyrin part), 3.64 (3H, s, 7^1-CH_3 – pyropheophorbide part), 3.66 (6H, m, $\beta-CH_3$ – coproporphyrin part), 3.88 (2H, q, J = 7.79 Hz, 8^1-CH_2 – pyropheophorbide part), 4.09 (3H, s, OCH_3), 4.23 (6H, m, OCH_2CH_3), 4.38 (9H, m, $CH_2CH_2CO_2Et$, 18-CH), 5.55 (1H, d, J = 19.58 Hz, 13^2-CH^b), 5.65 (1H, d, J = 19.58 Hz, 13^2-CH^a), 6.20 (1H, d, J = 11.64 Hz, 3^2-CH^b), 6.33 (1H, d, J = 18.00 Hz, 3^2-CH^a), 8.13 (1H, dd, J_1 = 18.00 Hz, J_2 = 11.64 Hz, 3^1-CH), 8.68 (1H, s, 20-CH – pyropheophorbide part), 9.69 (1H, s, 10-CH – pyropheophorbide part), 9.78 (1H, s, 5-CH – pyropheophorbide part), 10.09 (1H, s, 15-CH – coproporphyrin part), 10.13 (2H, s, 10,20-CH – coproporphyrin part), 11.42 (1H, s, CH=N). LDI TOF m/z : found 1443.05, calc. for $[M+H]^+$ $C_{79}H_{89}N_{10}O_{10}Pd$ 1443.58. UV-Vis (CH_2Cl_2) λ_{max} ($A_{rel.}$) nm: 399 (1.00), 514 (0.15), 550 (0.17), 620 (0.05), 678 (0.32).

Fluorescence lifetimes and quantum yields

Fluorescence lifetimes were measured by the time correlated single photon counting using a single photon counter PicoHarp TCSPC (PicoQuant GmbH). Excitation at 400 nm was performed with a LDH-P-C-405 laser head, and emission was registered at individual maximum for each compound. Excitation pulse frequency was set at 20 MHz for all tested compounds; excitation/detection bandpass 3 nm/2 nm, bin width 16 ps. In each case, the instrument response function (IRF) was recorded at the excitation wavelength with the Ludox scattering probe. Plots of the residuals showed random distributions in all cases. Fluorescence decays were fitted using a FluoFit software (PicoQuant GmbH). Fluorescence quantum yields were measured with a single photon counter TimeHarp TCSPC (PicoQuant GmbH), Xe Lamp (CW mode, bandwidth 2.7 nm, 1×0.4 cm quartz cuvette), with tetraphenylporphyrin (TPP) as a standard.

Singlet oxygen quantum yields measurements

Steady-state singlet oxygen phosphorescence measurements were carried out with NIR PMT Module H10330-45 (Hamamatsu) coupled to a single photon counter TimeHarp TCSPC (PicoQuant GmbH). Excitation at 400 nm was performed with the Xe Lamp (CW mode, bandwidth 5 nm, 1×0.4 cm quartz cuvette). Singlet oxygen quantum yields were determined in CH₂Cl₂ solutions, using TPP in benzene as a reference solution (Φ_{Δ} [TPP] = 0.62). Corrected emission spectra were recorded with the integration time 1 s between 1230 nm and 1330 nm. Total phosphorescence intensities were calculated by integrating the emission band centered at 1278 nm. Singlet oxygen quantum yield (Φ_{Δ}) values were determined using the equation $\Phi_{\Delta} = 0.62(I_{\Delta}/I_{\Delta r})$, where I_{Δ} and $I_{\Delta r}$ are singlet oxygen integrated emission intensities at 1230-1330 nm for tested compound and the reference, respectively. Φ_{Δ} measurements were performed in triplicate (standard deviation <10%).

Quantum-chemical calculations

Quantum-chemical calculations of geometry and electronic structure were made with the software package Gaussian 09W^[41] using density functional theory (DFT) method with the hybrid correlation-exchange functional B3LYP. A full-electron 6-31G(d,p) basis set was used for the geometry optimizations, electrons of nickel and palladium atoms were rendered by the basis set with an effective potential for internal electrons LaNL2DZ. The molecules were calculated in the chloroform solution using the polarized continuum (PCM) model. TD-DFT calculation of the electronic transitions were performed using WB97XD functional with DGDZVP basis set.

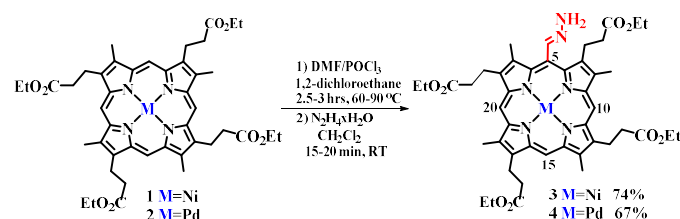
Results and Discussion

Synthesis

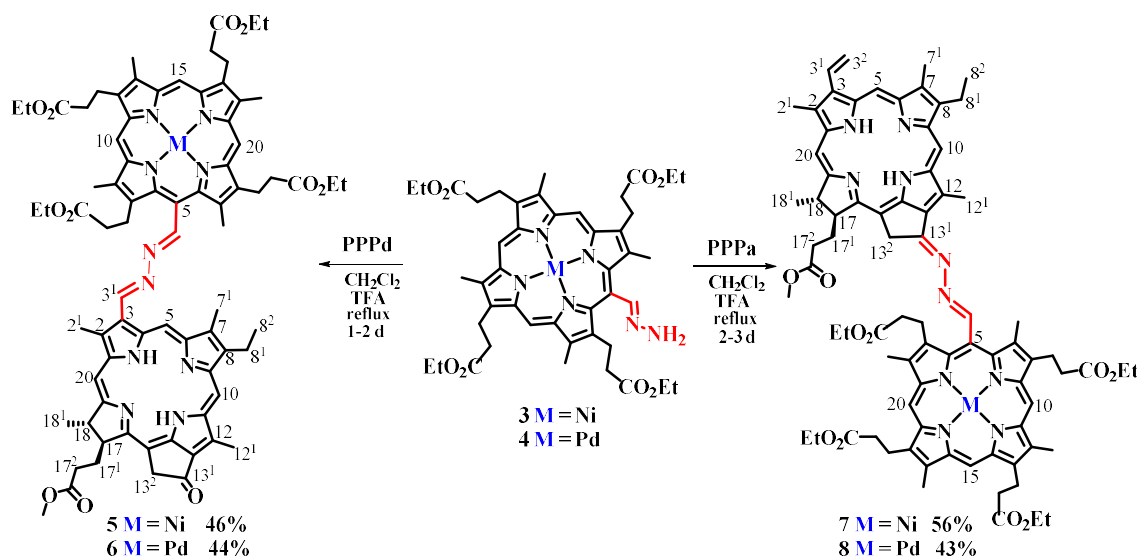
Components for preparation of dyads were chosen to be tetrapyrrolic compounds of two types: porphyrin and chlorin obtained from natural sources. Difference in the electronic levels of the units provide asymmetry in the dyad leading to processes of energy (electron) transfer between the fragments. Porphyrin component was tetraethyl ester of coproporphyrin I containing four ethyl ester protected carboxylic groups which facilitate aqueous solubility. Chlorin unit was one of natural chlorophyll *a* derivatives – pyropheophorbides *a* and *d*. Connection of parts into dyad with the azine bridge can be made with a reaction of a hydrazone derivative and carbonyl functionalized part. Pyropheophorbides already contain the carbonyl group which is necessary for the target azine bridge formation.

Coproporphyrin does not have a carbonyl group, which needs to be inserted. Previously, we have reported Vilsmeier's formylation of the metal porphyrins and subsequent reaction of the intermediately formed formyl derivatives with amines^[42,43] and hydrazines.^[38] The corresponding Schiff bases and hydrazones were obtained and their further transformations were investigated.^[44,45] The Vilsmeier-Haack formylation of porphyrins is usually performed with Ni^{II}, Cu^{II} or Pd^{II} complexes, as they are robust and stable, remaining intact under the acidic conditions of the formylation reaction. The four-coordinate state of the metal cations in these complexes provides their coordination saturation, leading to the absence of axial coordination of solvents and ligands, which can considerably affect their spectral properties. However, copper(II) porphyrins are paramagnetic which complicates their structure analysis by NMR. Therefore, palladium and nickel metals were chosen to be used in the porphyrin complexes. Both metals possess d8 electronic configuration in their dication form, however, Ni^{II} and Pd^{II} complexes differ dramatically upon light irradiation, and their comparison can be used for the photophysics study of the dyads. Pd significantly accelerates intersystem crossing due to the heavy atom effect, thus promoting the formation of triplet excited states,^[46] which is important for the phosphorescence and singlet oxygen generation processes used for photodynamic therapy.^[43,47] Meanwhile, nickel porphyrins direct the relaxation pathway of the excited state to the non-radiative internal conversion mechanism via fast (< 1 ps) formation of the nickel centered d-d excited state, and the latter returns back to the vibrationally excited ground state in 200-500 ps,^[48] thus converting light energy to the heat. Because of this, nickel complexes are considered for photothermal therapy.^[49]

The previously developed^[38] one-pot procedure for the synthesis of *meso*-hydrazones was applied to Ni^{II} and Pd^{II} complexes of the tetraethyl ester of coproporphyrin I. The Vilsmeier-Haack formylation with the Vilsmeier's reagent (formed from DMF and POCl₃) led to the formation of the intermediate *meso*-iminium salt, which was then subjected to the reaction with hydrazine hydrate. The first stage of electrophilic substitution of the Ni complex **1** proceeded at 60 °C temperature for 2.5 hrs while the electron poorer Pd complex **2** needed higher temperature of 90 °C and 3 hrs. The second stage of the reaction with hydrazine hydrate proceeded for 10-15 minutes at room temperature leading to the formation of an unsubstituted *meso*-hydrazones **3**, **4** with good total yield in two stages 74% and 67%, respectively (Scheme 1).



Scheme 1. Preparation of the *meso*-hydrazone derivatives of the coproporphyrin I.



Scheme 2. Synthesis of the dyads of pyropheophorbides with coproporphyrin I.

Meso-hydrazones of Ni^{II} and Pd^{II} complexes of the coproporphyrin I tetraethyl ester were then subjected to the interaction with methyl pyropheophorbide *a* (PPPa) and methyl pyropheophorbide *d* (PPPd) in refluxing dichloromethane, catalyzed by trifluoroacetic acid. As a result of the reaction, dyads combining pyropheophorbides with the metal coproporphyrin I derivatives with azine bridge were formed with good yields (Scheme 2).

Photophysical properties

In the UV-Vis absorption spectra of the pyropheophorbide-coproporphyrin dyads **5-8**, Q_y bands are bathochromically shifted compared to that of the electronically similar hydrazones of the corresponding methyl pyropheophorbide *d* (PPPd-N₂H₂)^[33] and methyl pyropheophorbide *a* (PPPa-N₂H₂)^[50] (Figure 1, Table 1). The maximum of the Q_y absorption band for dyads with pyropheophorbide *a* **7, 8** was shifted by 8–12 nm from 670 nm up to 682 nm, and for dyads with pyropheophorbide *d* **6, 7** was shifted by 18–19 nm from 676 nm up to 694–695 nm. The maxima of the Soret bands of the dyads are almost at the same place as that of the more intense Soret bands of the porphyrin component and showed almost no shift, remaining around 400 nm. However, a new shoulder of the Soret band arose at 430 nm. The less intense Q bands can also be attributed to one of the components. Thus the spectra of dyads can partly be considered as approximately a sum of spectra of components in the form of the corresponding hydrazones, however with an appreciable shift of the longest wavelength Q_y bands of the chlorin component. The bands of the chlorin component in the dyad are affected obviously more compared to that of the porphyrin component. This can be explained by rather a lack of π -electron coupling between the porphyrin macrocycle and azine bridge, which could be the consequence of their mutual orthogonal orientation due to the sterical hindrances at *meso*-position. Absence of such hindrances at β -position leads to the coplanar orientation and the corresponding π -electron conjugation of the azine bridge with the chlorin ring of the pyropheophorbides.

Table 1. UV-Vis absorption spectra data.

Compound	Absorption bands ^a		
	Soret band	Q _y band	
	λ_{\max} , nm	λ_{\max} , nm	I _{rel.} ^b
3	400	559	0.12
4	399	550	0.18
PPPd-N ₂ H ₂	413	676	0.76
PPPa-N ₂ H ₂	407	670	0.61
5	404	695	0.53
6	403	694	0.47
7	403	682	0.53
8	399	678	0.32

^a recorded in CH₂Cl₂ at concentration 10⁻⁵ M;

^b relative intensity of the Q_y band vs. the Soret band

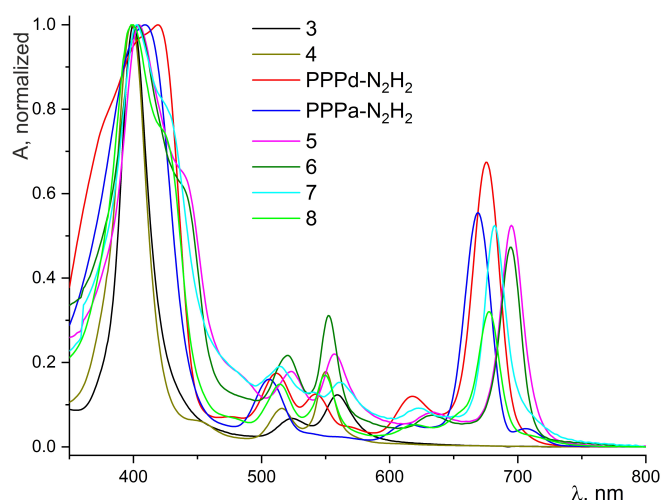


Figure 1. UV-Vis absorption spectra of the dyads **5-8** and their components **3, 4**, PPPd-N₂H₂, PPPa-N₂H₂. Spectra were recorded in CH₂Cl₂ at concentration of 10⁻⁵ M.

Photophysical studies of dyads revealed additional features of the interchromophore communication (Table 2). The fluorescence quantum yields Φ_f of the palladium dyads **6**, **8** are 18-19% with the lifetime τ_f of 4.5 ns whereas the nickel containing dyads **5**, **7** showed low fluorescence intensity with Φ_f equal about 1%. However, this value is significantly higher than that of the most of the nickel porphyrinates, which is usually less than 0.01%.^[51] Fast intersystem crossing processes, promoting by the heavy palladium atom, led to the transfer of the most of the excitation energy of the dyads **6**, **8** to the triplet state. This is manifested in the high enough quantum yields of the singlet oxygen generation $\Phi_{\Delta^1O_2}$ of 66-69%. The nickel dyads **5**, **7** gave also some singlet oxygen with 1-2% yield, which is also quite high for Ni porphyrinates possessing hardly detectible phosphorescence.^[51] The irradiation at 400 nm led to the possible excitation of both porphyrin and chlorin components of the dyads. The fluorescence spectra of dyads are close to that of the corresponding chlorin components (PPPa and PPPd) with a complete absence of porphyrin part emission (Figure 2). This fact is a consequence of the efficient excitation energy transfer from the palladium coproporphyrin to the chlorin component. Almost complete quenching of the fluorescence of the chlorin component by the linked nickel coproporphyrin additionally proves the considerable interaction between the components, as the excitation energy from the chlorin can fast enough be transferred to the coproporphyrin leading to the nickel *d-d* excited state and consequently to the excited vibrational states, as it was determined for Ni porphyrinates.^[46] Thus, the interaction of chromophores through the azine linker has apparently occurred in the excited state.

DFT studies of the structure of the dyads

In order to study the structure of the dyad molecules, quantum chemical calculations were performed using the DFT method. Optimization of the geometry of the molecules **5-8** in chloroform was performed by the B3LYP functional and 6-31G(d) basis set for light atoms and LanL2DZ for Ni. There were found two stable conformations of the Ni^{II} complexes with a little energy difference and one conformation of the Pd^{II} complexes. The only conformation of the Pd complex **8** and one conformation of the Ni^{II} complex **7** feature almost orthogonally oriented porphyrin rings with a little conjugation to each other (Figure 3A). Azine bridge is to some extent orthogonal to the nickel coproporphyrin plane, but is in plane with pyropheophorbide ring. The dihedral angle C-C-C-N between the C-C bond in the porphyrin cycle and C=N bond of azine is about 64° (for **7**). Analogous dihedral angle between the C-C bond of the pyropheophorbide and C=N bond of azine is 1°, and the angle around N-N bond is close to 180°. The second stable conformation of **7** has the azine bridge being partly conjugated to the coproporphyrin with the dihedral angle 29° and approximately coplanar tetrapyrrole macrocycles (Figure 3B). TD DFT calculations of the electron transitions using WB97XD functional and DGDZVP basis state showed that the longest wavelength absorption band

of approximately coplanar conformation was bathochromically shifted by 20 nm compared to that of the orthogonal conformation. Experimental UV-Vis spectra did not reveal this large enough shift, thus supporting the orthogonal conformation. Apart from that, the conjugation of the azine bridge to each component does not necessarily lead to the conjugation between the components due to the peculiarity of the azine group.^[33] Optimization of the geometry of **7** in the lowest singlet excited state by TD DFT with B3LYP functional and 6-31G(d) basis set revealed that the azine bridge was rotated to the lower dihedral angle to the porphyrin ring (Figure 3C). In the excited state S1 the angle of rotation of the bridge has been changed to the value of 7°. At the same time the porphyrin ring has been distorted lifting the azine bridge up relatively the ring plane, and tetrapyrrole planes of the dyad has become angled to each other (Figure 3C). Presumably, excited state drives interchromophore interaction up via increased conjugation which is in accordance with photophysical experiments.

Table 2. Results of the studies of the palladium complexes of dyads **6**, **8** in excited state.

Compound	λ_{abs} Q_y band, nm	λ_{em} ^a , nm	Φ_f ^{b,c} , %	τ_f , ns	$\Phi_{\Delta^1O_2}$ ^b , %
TPP ^d	646	649, 717	10		62
5	695	699	0.8		1
6	694	698, 750	18	4.5	69
7	682	685, 718	1.2		2
8	678	683, 723	19	4.5	66

^a Excitation at 400 nm in CH₂Cl₂ at concentration 10⁻⁶ M;

^b Reproducibility $\pm 10\%$;

^c The optical density is chosen to be equal for the tested and the reference compounds at the excitation wavelengths;

^d TPP – *meso*-tetraphenylporphyrin, used for comparison.

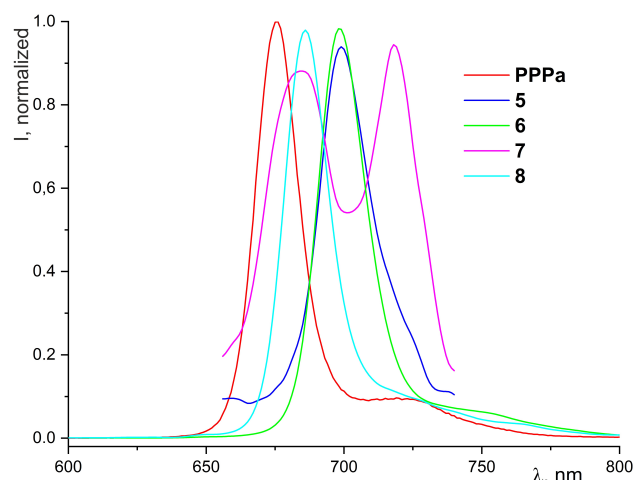


Figure 2. Normalized fluorescence spectra of the dyads **5-8** and methyl pyropheophorbide *a* (PPPa) recorded in CH₂Cl₂ at concentration of 10⁻⁶ M.

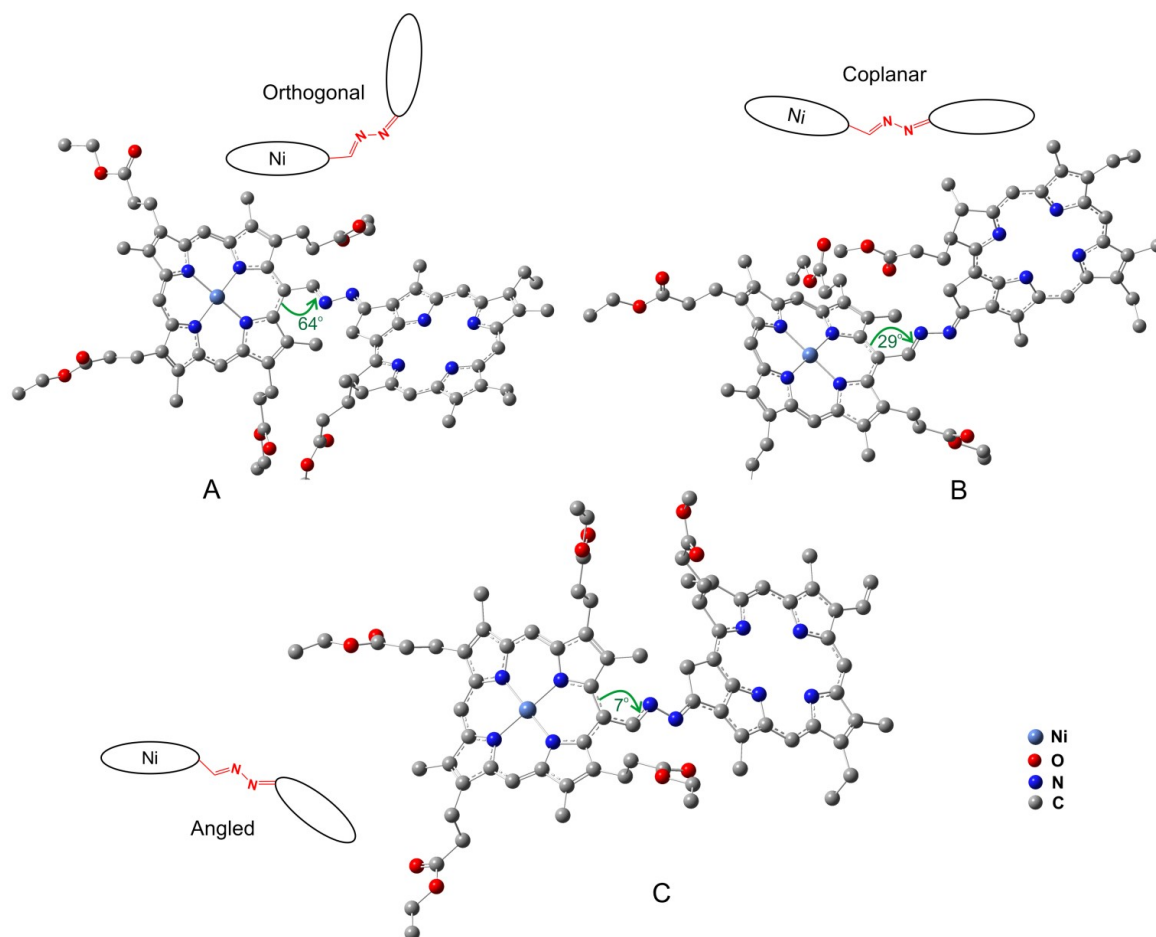


Figure 3. Geometry of the dyad 7 optimized by the DFT (B3LYP/6-31G(d)). Approximately orthogonal conformation (A), approximately coplanar conformation (B) and the optimized geometry of the excited S1 state (C). Hydrogen atoms are omitted for clarity.

In conclusion, new asymmetric dyads containing Ni^{II} and Pd^{II} coproporphyrin I and pyropheophorbides *a* and *d* were obtained. The UV-Vis spectra and DFT calculations showed a lack of conjugation between tetrapyrrole macrocycles in the ground state due to the mutual almost orthogonal orientation of the coproporphyrin ring and the azine bridge. However, efficient interchromophore communication arises in an excited state, as was deduced from the photophysical experiments and confirmed by the TD DFT calculations. The irradiation of palladium dyads resulted in the excited chlorin fragment, predominantly in triplet state, which is manifested in relatively high singlet oxygen generation quantum yields. Nickel complexes showed weak, but appreciable fluorescence and singlet oxygen generation, because the excited chlorin component did not completely quenched by the nickel porphyrinate component. The obtained dyads could be of interest as potential photosensitizers.

Acknowledgements. The reported study was funded by the Russian Science Foundation, grant 22-23-00903.

References

- Xiao L., Lai T., Liu X., Liu F., Russell T.P., Liu Y., Huang F., Peng X., Cao Y. *J. Mater. Chem. A* **2018**, *6*, 18469–18478. DOI: 10.1039/c8ta05903a.
- Watanabe M., Sun S., Ishihara T., Kamimura T., Nishimura M., Tani F. *ACS Appl. Energy Mater.* **2018**, *1*(11), 6072–6081. DOI: 10.1021/acsaem.8b01113.
- Kadish K., Guillard R., Smith K.M. *The Porphyrin Handbook: Multiporphyrins, Multiphthalocyanines and Arrays*. Elsevier Science, **2012**.
- Drobizhev M., Stepanenko Y., Dzenis Y., Karotki A., Rebane A., Taylor P.N., Anderson H.L. *J. Am. Chem. Soc.* **2004**, *126*, 15352–15353. DOI: 10.1021/ja0445847.
- Ohira S., Brédas J.-L. *J. Mater. Chem.* **2009**, *19*, 7545–7550. DOI: 10.1039/B906337D
- Balaz M., Collins H.A., Dahlstedt E., Anderson H.L. *Org. Biomol. Chem.* **2009**, *7*, 874–888. DOI: 10.1039/B814789B.
- Dahlstedt E., Collins H.A., Balaz M., Kuimova M.K., Khurana M., Wilson B.C., Phillips D., Anderson H.L. *Org. Biomol. Chem.* **2009**, *7*, 897–904. DOI: 10.1039/b814792b.
- Robbins E., Leroy-Lhez S., Villandier N., Samoć M., Matczyszyn K. *Molecules* **2021**, *26*, 6323. DOI: 10.3390/molecules26206323.
- Mohamed E.A., Zahran Z.N., Naruta Y. *J. Catal.* **2017**, *352*, 293–299. DOI: 10.1016/j.jcat.2017.05.018.
- Hammerer F., Garcia G., Charles P., Sourdon A., Achelle S., Teulade-Fichou M.-P., Maillard P. *Chem. Commun. (Cambridge, U. K.)* **2014**, *50*, 9529–9532. DOI: 10.1039/C4CC03367A.
- Tanasova M., Borhan B. *Eur. J. Org. Chem.* **2012**, *2012*(17), 3261–3269. DOI: 10.1002/ejoc.201200147.
- Beletskaya I., Tyurin V.S., Tsivadze A.Y., Guillard R., Stern C. *Chem. Rev.* **2009**, *109*, 1659–1713. DOI: 10.1021/cr800247a.

13. Koifman O.I., Ageeva T.A. *Russ. J. Org. Chem.* **2022**, *58*, 443–479. DOI: 10.1134/S1070428022040017.
14. Tyurin V.S., Uglov A., Beletskaya I.P., Stern C., Guillard R. In: *Handbook of Porphyrin Science, Vol. 23* (Kadish K.M., Smith K.M., Guillard R., Eds.), World Scientific: Singapore, **2012**, Ch. 108, pp. 81–279.
15. Vicente M.d.G.H., Smith K.M. *Curr. Org. Synth.* **2014**, *11*, 3–28. DOI: 10.2174/15701794113106660083.
16. Senge M.O. *Chem. Commun.* **2011**, *47*, 1943–1960. DOI: 10.1039/C0CC03984E.
17. Kim S.-H., Gwon S.-Y., Burkinshaw S.M., Son Y.-A. *Dyes Pigm.* **2010**, *87*, 268–271. DOI: 10.1016/j.dyepig.2010.04.006.
18. Gunnlaugsson T., Leonard J.P., Murray N.S. *Org. Lett.* **2004**, *6*, 1557–1560. DOI: 10.1021/ol0498951.
19. Sheng R., Wang P., Liu W., Wu X., Wu S. *Sens. Actuators, B* **2008**, *128*, 507–511 DOI: 10.1016/j.snb.2007.07.069.
20. Tang W., Xiang Y., Tong A. *J. Org. Chem.* **2009**, *74*, 2163–2166. DOI: 10.1021/jo802631m.
21. McLoughlin C., Clyburne J.A.C., Weinberg N. *J. Mater. Chem.* **2007**, *17*, 4304–4308. DOI: 10.1039/b706964b.
22. Choytun D.D., Langlois L.D., Johansson T.P., Macdonald C.L.B., Leach G.W., Weinberg N., Clyburne J.A.C. *Chem. Commun.* **2004**, *2004*(16), 1842–1843. DOI: 10.1039/b404129a.
23. Vercelli B., Pasini M., Berlin A., Casado J., Lopez Navarrete J.T., Ortiz R.P., Zotti G. *J. Phys. Chem. C* **2014**, *118*, 3984–3993. DOI: 10.1021/jp411815w.
24. Poduval M.K., Arrechea-Marcos I., Carmen Ruiz Delgado M., Park T., Lopez Navarrete J.T., Ortiz R.P., Kim T.-H. *RSC Adv.* **2016**, *6*, 44272–44278. DOI: 10.1039/C6RA07389A.
25. Khodair A.I., Bertrand P. *Tetrahedron* **1998**, *54*, 4859–4872. DOI: 10.1016/S0040-4020(98)00170-7.
26. Sun C.-W., Wang H.-F., Zhu J., Yang D.-R., Xing J., Jin J. *J. Heterocycl. Chem.* **2013**, *50*, 1374–1380. DOI: 10.1002/jhet.916.
27. Iwan A., Rannou P., Janeczka H., Palewicz M., Hreniak A., Bilski P., Oswald F., Pocięcha D. *Synth. Met.* **2010**, *160*, 859–865. DOI: 10.1016/j.synthmet.2010.01.035.
28. Tindale J.J., Holm H., Workentin M.S., Semenikhin O.A. *J. Electroanal. Chem.* **2008**, *612*, 219–230. DOI: 10.1016/j.jelechem.2007.10.003.
29. Ardaraviciene J., Barvainiene B., Malinauskas T., Jankauskas V., Arlauskas K., Getautis V. *React. Funct. Polym.* **2011**, *71*, 1016–1022. DOI: 10.1016/j.reactfunctpolym.2011.07.005.
30. Kwon O., Choo J., Kim S., Kwon Y. *THEOCHEM* **2004**, *685*, 185–189. DOI: 10.1016/j.theochem.2004.06.046.
31. Safari J., Gandomi-Ravandi S. *RSC Advances* **2014**, *4*, 46224–46249. DOI: 10.1039/c4ra04870a.
32. Orlova E.A., Romanenko Y.I., Tyurin V.S., Shkirdova A.O., Belyaev E.S., Grigoriev M.S., Koifman O.I., Zamilatskov I.A. *Macromolecules* **2022**, *15*, 139–146. DOI: 10.6060/mhc224638z.
33. Belyaev E.S., Shkirdova A.O., Kozhemyakin G.L., Tyurin V.S., Emets V.V., Grinberg V.A., Cheshkov D.A., Ponomarev G.V., Tafeenko V.A., Radchenko A.S., Kostyukov A.A., Egorov A.E., Kuzmin V.A., Zamilatskov I.A. *Dyes Pigm.* **2021**, *191*, 109354. DOI: 10.1016/j.dyepig.2021.109354.
34. Andreeva V.D., Ponomarev G.V., Shkirdova A.O., Tyurin V.S., Zamilatskova I.A. *Macromolecules* **2021**, *14*, 201–207. DOI: 10.6060/mhc213990z.
35. Tamiaki H., Amakawa M., Shimono Y., Tanikaga R., Holzwarth A.R., Schaffner K. *Photochem. Photobiol.* **1996**, *63*, 92–99. DOI: 10.1111/j.1751-1097.1996.tb02997.x.
36. Johnson D.G., Svec W.A., Wasielewski M.R. *Isr. J. Chem.* **1988**, *28*, 193–203. DOI: 10.1002/ijch.198800030.
37. Smith K.M. *J. Chem. Soc., Perkin Trans. 1* **1972**, 1471–1475. DOI: 10.1039/P19720001471.
38. Shkirdova A.O., Zamilatskov I.A., Stanetskaya N.M., Tafeenko V.A., Tyurin V.S., Chernyshev V.V., Ponomarev G.V., Tsvadze A.Y. *Macromolecules* **2017**, *10*, 480–486. DOI: 10.6060/mhc171148z.
39. Adler A.D., Longo F.R., Kampas F., Kim J. *J. Inorg. Nucl. Chem.* **1970**, *32*, 2443–2445. DOI: 10.1016/0022-1902(70)80535-8.
40. Kalisch W.W., Senge M.O., Ruhlandt-Senge K. *Photochem. Photobiol.* **1998**, *67*, 312–323. DOI: 10.1111/j.1751-1097.1998.tb05204.x.
41. Frisch M.J., Trucks G.W., Schlegel H.B., Scuseria G.E., Robb M.A., Cheeseman J.R., Scalmani G., Barone V., Mennucci B., Petersson G.A., Nakatsuji H., Caricato M., Li X., Hratchian H.P., Izmaylov A.F., Bloino J., Zheng G., Sonnenberg J.L., Hada M., Ehara M., Toyota K., Fukuda R., Hasegawa J., Ishida M., Nakajima T., Honda Y., Kitao O., Nakai H., Vreven T., Montgomery J.A.J., Peralta J.E., Ogliaro F., Bearpark M., Heyd J.J., Brothers E., Kudin K.N., Staroverov V.N., Keith T., Kobayashi R., Normand J., Raghavachari K., Rendell A., Burant J.C., Iyengar S.S., Tomasi J., Cossi M., Rega N., Millam J.M., Klene M., Knox J.E., Cross J.B., Bakken V., Adamo C., Jaramillo J., Gomperts R., Stratmann R.E., Yazyev O., Austin A.J., Cammi R., Pomelli C., Ochterski J.W., Martin R.L., Morokuma K., Zakrzewski V.G., Voth G.A., Salvador P., Dannenberg J.J., Dapprich S., Daniels A.D., Farkas O., Foresman J.B., Ortiz J.V., Cioslowski J., Fox D.J. *Gaussian 09, Revision D.01*, Gaussian, Inc., Wallingford CT, **2013**.
42. Volov A.N., Zamilatskov I.A., Mikhel I.S., Erzina D.R., Ponomarev G.V., Koifman O.I., Tsvadze A.Y. *Macromolecules* **2014**, *7*, 256–261. DOI: 10.6060/mhc140274z.
43. Tyurin V.S., Erzina D.R., Zamilatskov I.A., Chernyadyev A.Y., Ponomarev G.V., Yashunskiy D.V., Maksimova A.V., Krasnovskiy A.A., Tsvadze A.Y. *Macromolecules* **2015**, *8*, 376–383. DOI: 10.6060/mhc151199z.
44. Erzina D.R., Zamilatskov I.A., Stanetskaya N.M., Tyurin V.S., Kozhemyakin G.L., Ponomarev G.V., Chernyshev V.V., Fitch A.N. *Eur. J. Org. Chem.* **2019**, *2019*(7), 1508–1522. DOI: 10.1002/ejoc.201801659.
45. Kozhemyakin G.L., Tyurin V.S., Shkirdova A.O., Belyaev E.S., Kirinova E.S., Ponomarev G.V., Chistov A.A., Aralov A.V., Tafeenko V.A., Zamilatskov I.A. *Org. Biomol. Chem.* **2021**, *19*, 9199–9210. DOI: 10.1039/D1OB01626A.
46. Kobayashi T., Straub K.D., Rentzepis P.M. *Photochem. Photobiol.* **1979**, *29*, 925–931 DOI: 10.1111/j.1751-1097.1979.tb07793.x.
47. Borisov S.M., Papkovsky D.B., Ponomarev G.V., De Toma A.S., Saf R., Klimant I. *J. Photochem. Photobiol., A* **2009**, *206*, 87–92. DOI: 10.1016/j.jphotochem.2009.05.018.
48. Chirvonyi V.S., Dzhagarov B.M., Timinskii Y.V., Gurinovich G.P. *Chem. Phys. Lett.* **1980**, *70*, 79–83. DOI: 10.1016/0009-2614(80)80064-9.
49. Camerin M., Rello S., Villanueva A., Ping X., Kenney M.E., Rodgers M.A.J., Jori G. *Eur. J. Cancer* **2005**, *41*, 1203–1212. DOI: 10.1016/j.ejca.2005.02.021.
50. Lonin I.S., Belyaev E.S., Tsvadze A.Y., Ponomarev G.V., Lonina N.N., Fitch A.N., Chernyshev V.V. *Macromolecules* **2017**, *10*, 474–479. DOI: 10.6060/mhc170832l.
51. Harriman A. *J. Chem. Soc., Faraday Trans. 1* **1980**, *76*, 1978–1985. DOI: 10.1039/F19807601978.

Received 27.03.2023

Accepted 23.04.2023